Deep-Core Dielectronic-Capture Resonances in the Electron-Impact Ionization of Heavy Atomic Ions

K. Aichele, D. Hathiramani, F. Scheuermann, A. Müller, and E. Salzborn
Institut für Kernphysik, Justus-Liebig-Universität Giessen, D-35392 Giessen, Germany

D. Mitnik, J. Colgan, and M. S. Pindzola
Department of Physics, Auburn University, Auburn, Alabama 36849
(Received 6 September 2000)

Experimental measurements and theoretical calculations are carried out for the electron-impact ionization of Sm^{12+}. The low energy region of the single ionization cross section for Sm^{12+} is found to be dominated by contributions from the indirect process of excitation autoionization. At about 1.0 keV strong resonance features are found in the experimental crossed-beam measurements performed in scan mode at high resolution. Theoretical calculations confirm that the high energy experimental features are due to deep-core dielectronic capture followed by sequential double Auger decay. The discovery of these unusual high energy resonances in single and multiple ionization opens the door for future systematic studies of how heavy atomic ions with deep inner-shell vacancies achieve final stabilization.

DOI: 10.1103/PhysRevLett.86.620 PACS numbers: 34.80.Dp, 34.70.+e

One of the most important atomic collision processes in a microscopic description of many laboratory and astrophysical plasmas is the electron-impact ionization of an atomic ion. For light ions the dominant mechanism for single ionization is the same direct knockout process which is the sole mechanism in the electron-impact ionization of the hydrogen atom. For moderate to heavy ions substantial contributions to single ionization are made by indirect ionization processes which make use of the shell structure of the atomic ion. The indirect process of the excitation of an inner-shell electron followed by single autoionization is found to dominate the total single ionization cross section for many ions, especially for those targets with one or two electrons outside a closed $l \geq 1$ subshell. This excitation-autoionization process is generally characterized by a steplike feature in the total ionization cross section. The additional indirect process of simultaneous excitation of an inner-shell electron and capture of the incident electron followed by sequential double autoionization is also found to make a substantial contribution to the total single ionization cross section for many of those same ions. This dielectronic capture process is generally characterized by a series of resonances converging to the steplike threshold of an excitation-autoionization feature. The acronym REDA (resonant excitation double autoionization) was first coined by LaGattuta and Hahn [1] to describe these resonance features in the single ionization of Fe^{15+}.

Over the last 12 years dielectronic capture resonances have been experimentally observed in the electron-impact ionization of quite a few atomic ions. For Li-like ions experimental crossed-beam measurements have mapped out resonance structures for B^{2+} to F^{6+} [2–5]. Theoretical calculations [4–8] using close-coupling and distorted-wave methods are found to accurately reproduce most of the detailed resonance patterns for these light Li-like ions. Theoretical predictions [9,10] for resonances in more highly charged Li-like ions have been confirmed by ion storage ring experiments for Si^{11+} and Cl^{14+} [11]. For Na-like ions crossed-beam measurements have mapped out resonance structures for Mg^{+} [12,13] and Al^{2+} [14]; however, theoretical close-coupling calculations [15–17] are not as accurate in predicting the resonance details. A number of theoretical predictions [1,18,19] were made for resonance structures in Fe^{15+}. Ion storage ring measurements [20] are in substantial agreement with the theoretical predictions but differ as to the rich detail found in the resonance structures. Theoretical predictions [21] for resonances in more highly charged Na-like ions have also been made, with only limited confirmation by ion storage ring measurements for Se^{23+} [22]. For low-charged heavy metal ions crossed-beam measurements have mapped out large and complex resonance structures for Cs^{+}, Ba^{2+}, Ba^{3+}, La^{2+}, and La^{3+} [23–25]; however, no theoretical resonance calculations yet exist.

All the dielectronic capture resonances previously observed may be identified with simultaneous excitation of the "nearest" shell electron and capture of the incident electron. For example,

$$e^{-} + C^{3+}(1s^2 2s) \rightarrow C^{2+}(1s2snln'l'),$$

$$e^{-} + Fe^{15+}(2p^6 3s) \rightarrow Fe^{14+}(2p^5 3snln'l'),$$

$$e^{-} + La^{3+}(4d^{10}5s^2 5p^6) \rightarrow La^{2+}(4d^9 5s^2 5p^6 nln'l').$$

These resonance features strongly overlap the largest excitation-autoionization contributions coming from

$$e^{-} + C^{3+}(1s^2 2s) \rightarrow C^{3+}(1s2s2p) + e^{-},$$

$$e^{-} + Fe^{15+}(2p^6 3s) \rightarrow Fe^{15+}(2p^5 3s3p) + e^{-},$$

$$e^{-} + La^{3+}(4d^{10}5s^2 5p^6) \rightarrow La^{3+}(4d^9 5s^2 5p^6 4f) + e^{-}.$$

Thus, the total indirect ionization contribution for these ions is a blend of both resonant and steplike features on a smooth direct ionization background.

 0031-9007/01/86(4)/620(4)$15.00

In this Letter we report on the discovery of isolated resonances on a smooth background at high incident energy for many single ionization cross sections of atomic ions with charge states up to 13+ in the Pr and Sm rare earth isonuclear sequences. These unusual resonances are well above the threshold energies associated with the major direct and indirect contributions to single ionization of the particular target ion. In fact, the resonances are well above the triple and even quadruple ionization thresholds of the atomic ion. They are clearly seen only when we perform our crossed-beam experiment in scan mode at high resolution. As comparison with theoretical calculations for resonance energies and autoionization rates will show, we identify these high energy resonance features with a dielectronic capture process involving a deep core inner-subshell electron. The same high energy resonance is found in the single, double, and even triple ionization cross section of the target ion. The resonance peak area in the various multiple ionization cross sections is related to the relative strengths of the various decay paths available to an ion with a deep core inner-shell vacancy.

An example of our findings and a clear illustration of these high energy resonances are found in the electron-impact ionization of Sm^{12+}. We present an energy level diagram for some of the transitions involving the $4d$ electron starting from the $4d^{10}4f^25s^2$ ground configuration of Sm^{12+} in Fig. 1. Direct ionization of the $5s$, $4f$, $4d$, and $4p$ subshells leads to the single ionization of Sm^{12+}. Direct ionization of the $4s$ subshell leads to double ionization of Sm^{12+}. The $4d \rightarrow 4f$ excitation leads to bound states of Sm^{12+}, while the $4d \rightarrow 5f$ and $4d \rightarrow 6l$ excitations lead to autoionizing states of Sm^{12+} and thus contribute to single ionization. Finally $4d \rightarrow nl$ excitation with simultaneous capture of the incident electron into an $n'l'$ subshell leads to resonance structures in the single ionization of Sm^{12+} at low energies.

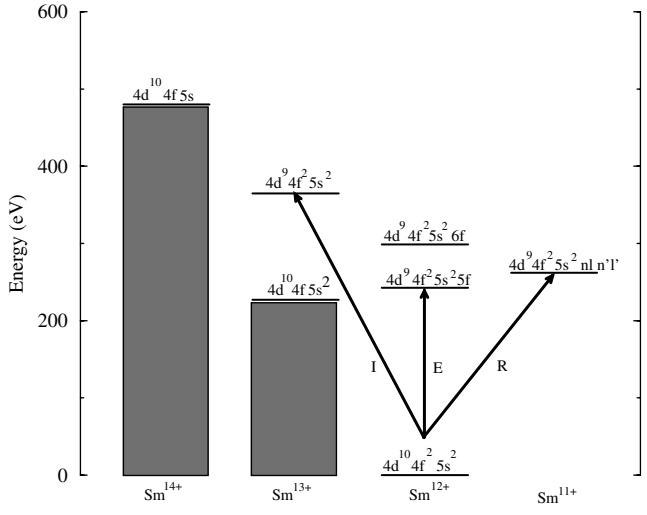

FIG. 1. Energy level diagram for the transitions involving the $4d$ electron out of the $4d^{10}4f^25s^2$ ground configuration of Sm^{12+}. Lines marked R involve dielectronic capture, lines marked E involve excitation, and lines marked I involve direct ionization. The $1s$, $2s$, $2p$, $3s$, $3p$, $3d$, $4s$, and $4p$ subshells are assumed filled.

We present experimental crossed-beam measurements (see Müller *et al.* [5] for details) and configuration-average distorted-wave calculations (see Pindzola *et al.* [26] for details) for the single ionization cross section of Sm^{12+} in Fig. 2. The total cross section from 200 to 500 eV is dominated by contributions from excitation autoionization, the largest due to $4d \rightarrow 5f$, $4d \rightarrow 6l$, $4p \rightarrow 4f$, and $4p \rightarrow 5l$ transitions. The measurements for the single ionization of Sm^{12+} lie above the configuration-average distorted-wave calculations for total ionization from the $4d^{10}4f^25s^2$ ground configuration across the entire energy range. However, the measurements lie slightly below the theoretical calculations for total ionization from the $4d^{10}4f^4$ excited configuration at energies above 500 eV. Although not shown in Fig. 2, the theoretical calculations for total ionization from the $4d^{10}4f^35s$ excited configuration fall between the $4d^{10}4f^25s^2$ and $4d^{10}4f^4$ results. As found before in many crossed-beam experiments with complex ions [27–29], the ion beam is an unknown mixture of the ground level of the ground configuration and the many long-lived metastable levels found in the ground and low-lying excited configurations. We note that part of the shortfall in the theoretical predictions for energies below 500 eV may be due to contributions from $4d \rightarrow nl$ dielectronic capture resonances that were not included.

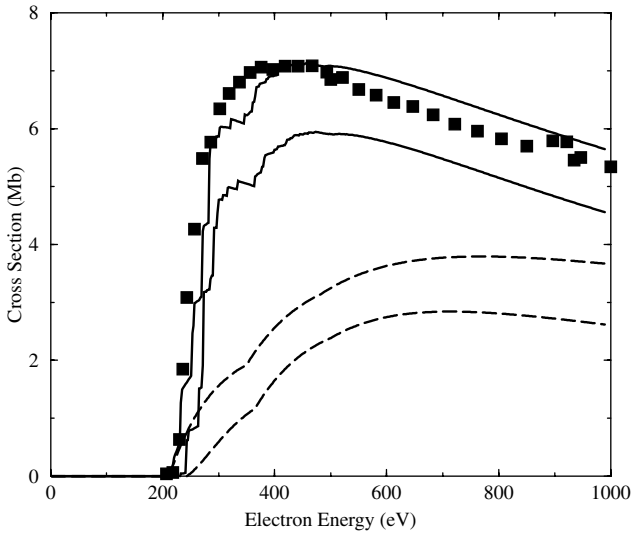

FIG. 2. Electron-impact ionization of Sm^{12+}. Lower solid line: direct ionization and excitation autoionization from the $4d^{10}4f^25s^2$ ground configuration, upper solid line: direct ionization and excitation autoionization from the $4d^{10}4f^4$ excited configuration, lower dashed curve: direct ionization only from the $4d^{10}4f^25s^2$ ground configuration, upper dashed curve: direct ionization only from the $4d^{10}4f^4$ excited configuration, and solid squares: experimental measurements for single ionization. The statistical uncertainties of the experimental data are within the size of the symbols. Systematic uncertainties of the measurements are below 10%. 1.0 Mb = 1.0×10^{-18} cm^2.

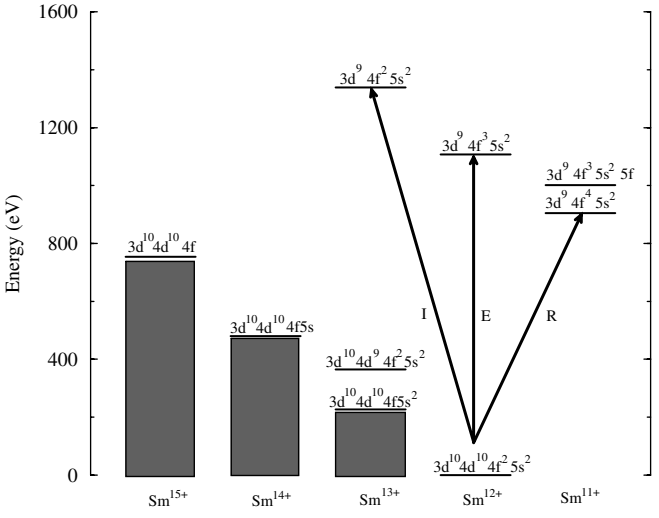

FIG. 3. Energy level diagram for the transitions involving the $3d$ electron out of the $3d^{10}4f^{2}5s^{2}$ ground configuration of Sm^{12+}. Lines marked R involve dielectronic capture, lines marked E involve excitation, and lines marked I involve direct ionization. The $1s$, $2s$, $2p$, $3s$, $3p$, $4s$, $4p$, and $4d$ subshells are assumed filled.

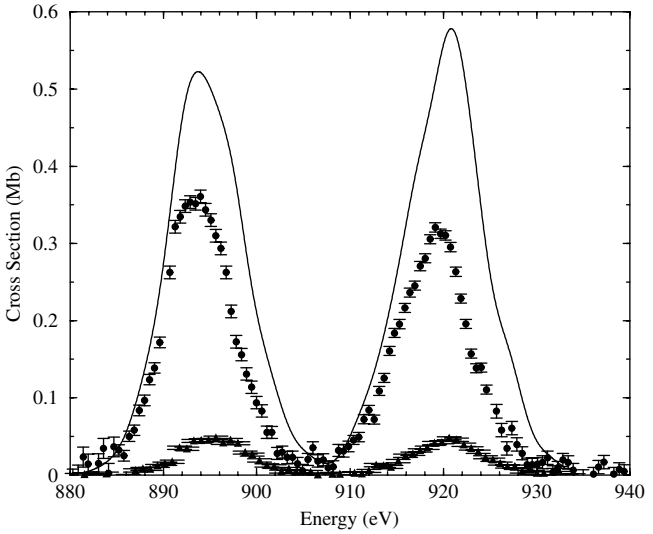

FIG. 4. Electron-impact ionization of Sm^{12+}. Solid line: dielectronic capture to the $3d^{9}4f^{4}5s^{2}$ excited configuration, solid circles: experimental measurements for single ionization, and solid triangles: experimental measurements for double ionization. 1.0 Mb = 1.0×10^{-18} cm^2.

The unusual features represented by the two experimental points around an incident energy of 900 eV in Fig. 2 prompted further experimental and theoretical investigation. We present an energy level diagram for some of the transitions involving the $3d$ electron starting from the $4d^{10}4f^{2}5s^{2}$ ground configuration of Sm^{12+} in Fig. 3. Direct ionization of the $3d$ subshell is well above the triple ionization threshold of Sm^{12+}. The $3d \rightarrow 4f$ excitation leads to high-lying autoionizing states of Sm^{12+} which most likely contribute to the double ionization of Sm^{12+} by sequential double autoionization. Finally, the $3d \rightarrow 4f$ excitation with simultaneous capture of the incident electron into the $4f$ subshell results in an excited configuration of Sm^{11+} which lies 905 eV above the $4d^{10}4f^{2}5s^{2}$ ground configuration of Sm^{12+}. A possible sequential double autoionization here would result in single ionization of Sm^{12+}, and thus an answer to the mystery of the two unusual points in Fig. 2.

We present experimental crossed-beam measurements, performed in scan mode at high resolution from 880 to 940 eV, for the single and double ionization cross section of Sm^{12+} in Fig. 4. To focus on the resonance features, the smooth experimental background cross sections for both single and double ionization have been subtracted out. Configuration-average distorted-wave calculations for the dielectronic capture strength are presented in Table I. By far the largest capture strength is from the $3d^{10}4f^{2}5s^{2}$ ground configuration of Sm^{12+} to the $3d^{9}4f^{4}5s^{2}$ resonance configuration of Sm^{11+}. The next largest capture strength is from the $3d^{10}4f^{4}$ excited configuration of Sm^{12+} to the $3d^{9}4f^{6}$ resonance configuration of Sm^{11+}. Although not shown in Table I, the capture strengths from the $3d^{10}4f^{3}5s$ excited configuration of Sm^{12+} are dominated by the transition to the $3d^{9}4f^{5}5s$ resonance configuration of Sm^{11+} at 909 eV. Thus, in the experimental energy range of Fig. 4 there are over 3000 fine structure levels associated with the $3d^{9}4f^{4}5s^{2}$, $3d^{9}4f^{5}5s$, and $3d^{9}4f^{6}$ resonance configurations centered at about 910 eV, but actually spread over approximately 60 eV.

As a simple first estimate, we carried out level to level distorted-wave calculations (see Oreg *et al.* [30] for details) for the dielectronic capture strength from an average over the 12 levels of the $3d^{10}4f^{2}5s^{2}$ ground configuration of Sm^{12+} to each of the 977 levels of the $3d^{9}4f^{4}5s^{2}$ excited configuration of Sm^{11+}. We shift the entire 60 eV wide spectrum by 8.0 eV, which is entirely within that expected from configuration interaction in the $3d$ subshell of a heavy atom, and then fold the dielectronic capture strength with a 3.0 eV Gaussian distribution representing the experimental energy resolution. As found in Fig. 4, our

TABLE I. Dielectronic capture strengths for $e^- + Sm^{12+} \rightarrow Sm^{11+}$. The $1s$, $2s$, $2p$, $3s$, $3p$, $4s$, $4p$, and $4d$ subshells are assumed filled. 1.0 Mb = 1.0×10^{-18} cm^2.

Initial configuration	Final configuration	Energy (eV)	Strength (Mb × eV)
$3d^{10}4f^{2}5s^{2}$	$3d^{9}4f^{4}5s^{2}$	905	13.3
	$3d^{9}4f^{3}5s^{2}5p$	918	0.24
	$3d^{9}4f^{3}5s^{2}5d$	959	1.89
	$3d^{9}4f^{3}5s^{2}5f$	1001	5.94
	$3d^{9}4f^{3}5s^{2}5g$	1026	0.06
$3d^{10}4f^{4}$	$3d^{9}4f^{5}5s$	893	0.22
	$3d^{9}4f^{6}$	913	7.56
	$3d^{9}4f^{5}5p$	920	0.17
	$3d^{9}4f^{5}5d$	958	1.36
	$3d^{9}4f^{5}5f$	997	4.42
	$3d^{9}4f^{5}5g$	1021	0.04

simple estimate is in reasonable agreement with the experimental measurements. The bimodal cross section distribution is due to the approximately 25.8 eV spin-orbit splitting found in the $3d^9$ subshell of Sm^{11+}. It should be noted that dielectronic capture is only the first step to many final outcomes: recombination, resonant elastic and inelastic scattering, single ionization, double ionization, and even triple ionization. For example, the branching ratio for single ionization involves the sequential double autoionization given by

$$\begin{aligned} Sm^{11+}(3d^9 4s^2 4p^6 4d^{10} 4f^4 5s^2) &\rightarrow Sm^{12+}(3d^{10} 4s^2 4p^5 4d^9 4f^4 5s^2) + e^- \\ &\downarrow \\ &\quad Sm^{13+}(3d^{10} 4s^2 4p^6 4d^9 4f^2 5s^2) + e^-. \end{aligned}$$

A full level to level single configuration distorted-wave calculation for the single ionization branching ratio involves hundreds of thousands of radiative and autoionization rates to ground, excited, and resonance configurations of Sm^{11+} through Sm^{15+}. Certainly, the configuration-interaction level to level distorted-wave calculation needed to accurately map out the deep-core dielectronic capture resonances found in the ionization of Sm^{12+} is a daunting computational challenge.

In summary, strong resonance features near 1.0 keV incident energy are found in experimental crossed-beam measurements of the electron-impact ionization of Sm^{12+}. Theoretical calculations of resonance energies and autoionization rates confirm that the high energy experimental features are due to deep-core dielectronic capture followed by sequential Auger decay. The same unusual high energy resonances are found in many other single and multiple ionization measurements with heavy atomic ions. Their discovery opens the door for future experimental and theoretical studies of how heavy atomic ions with deep inner-shell vacancies achieve final stabilization.

This work was supported in part by the Deutsche Forschungsgemeinschaft and by the U.S. Department of Energy. Computational work was carried out at the National Energy Research Supercomputer Center in Berkeley, CA, and VW-Stiftung.

[1] K. J. LaGattuta and Y. Hahn, Phys. Rev. A **24**, 2273 (1981).
[2] A. Müller, G. Hofmann, K. Tinschert, and E. Salzborn, Phys. Rev. Lett. **61**, 1352 (1988).
[3] G. Hofmann, A. Müller, K. Tinschert, and E. Salzborn, Z. Phys. D **16**, 113 (1990).
[4] H. Teng, H. Knopp, S. Ricz, S. Schippers, K. A. Berrington, and A. Müller, Phys. Rev. A **61**, 060704(R) (2000).
[5] A. Müller, H. Teng, G. Hofmann, R. A. Phaneuf, and E. Salzborn, Phys. Rev. A **62**, 062720 (2000).
[6] S. S. Tayal and R. J. W. Henry, Phys. Rev. A **44**, 2955 (1991).
[7] K. J. Reed and M. H. Chen, Phys. Rev. A **45**, 4519 (1992).
[8] M. P. Scott, H. Teng, and P. G. Burke, J. Phys. B **33**, L63 (2000).
[9] M. H. Chen and K. J. Reed, Phys. Rev. A **45**, 4525 (1992).
[10] N. R. Badnell and M. S. Pindzola, Phys. Rev. A **47**, 2937 (1993).
[11] J. Kenntner, J. Linkemann, N. R. Badnell, C. Broude, D. Habs, G. Hofmann, A. Müller, M. S. Pindzola, E. Salzborn, D. Schwalm, and A. Wolf, Nucl. Instrum Methods Phys. Res., Sect. B **98**, 142 (1995).
[12] A. Müller, G. Hofmann, K. Tinschert, B. Weissbecker, and E. Salzborn, Z. Phys. D **15**, 145 (1990).
[13] B. Peart, J. W. G. Thomason, and K. Dolder, J. Phys. B **24**, 4453 (1991).
[14] J. W. G. Thomason and B. Peart, J. Phys. B **31**, L201 (1998).
[15] S. S. Tayal, J. Phys. B **24**, L219 (1991).
[16] Z. Felfli, K. A. Berrington, and A. Msezane, J. Phys. B **33**, 1263 (2000).
[17] H. Teng, J. Phys. B **33**, L553 (2000).
[18] S. S. Tayal and R. J. W. Henry, Phys. Rev. A **39**, 3890 (1989).
[19] M. H. Chen, K. J. Reed, and D. L. Moores, Phys. Rev. Lett. **64**, 1350 (1990).
[20] J. Linkemann, A. Müller, J. Kenntner, D. Habs, D. Schwalm, A. Wolf, N. R. Badnell, and M. S. Pindzola, Phys. Rev. Lett. **74**, 4173 (1995).
[21] M. H. Chen and K. J. Reed, Phys. Rev. A **47**, 1874 (1993).
[22] J. Linkemann, A. Müller, W. Spies, O. Uwira, A. Frank, T. Cramer, J. Kenntner, A. Wolf, C. Broude, D. Habs, D. Schwalm, G. H. Dunn, N. R. Badnell, and M. S. Pindzola, in Stuttgart Inst. Rad. Phys. Annual Report No. 5, 1995, edited by R. Kunz and H. H. Pitz (unpublished), p. 34.
[23] A. Müller, K. Tinschert, G. Hofmann, E. Salzborn, and G. H. Dunn, Phys. Rev. Lett. **61**, 70 (1988).
[24] A. Müller, K. Tinschert, G. Hofmann, E. Salzborn, G. H. Dunn, S. M. Younger, and M. S. Pindzola, Phys. Rev. A **40**, 3584 (1989).
[25] K. Tinschert, A. Müller, G. Hofmann, E. Salzborn, and S. M. Younger, Phys. Rev. A **43**, 3522 (1991).
[26] M. S. Pindzola, D. C. Griffin, and C. Bottcher, in *Atomic Processes in Electron-Ion and Ion-Ion Collisions,* NATO ASI, Ser. B, Vol. 145 (Plenum Press, New York, 1986), p. 75.
[27] D. Hathiramani, K. Aichele, G. Hofmann, M. Steidl, M. Stenke, R. Volpel, E. Salzborn, M. S. Pindzola, J. A. Shaw, D. C. Griffin, and N. R. Badnell, Phys. Rev. A **54**, 587 (1996).
[28] U. Hartenfeller, K. Aichele, D. Hathiramani, G. Hofmann, V. Schafer, M. Steidl, M. Stenke, E. Salzborn, and M. S. Pindzola, J. Phys. B **31**, 2999 (1998).
[29] J. A. Shaw, M. S. Pindzola, M. Steidl, K. Aichele, U. Hartenfeller, D. Hathiramani, F. Scheuermann, M. Westermann, and E. Salzborn, Phys. Rev. A (to be published).
[30] J. Oreg, W. H. Goldstein, M. Klapisch, and A. Bar-Shalom, Phys. Rev. A **44**, 1750 (1991).